Multi-Response Optimisation of Automotive Door Using Grey Relational Analysis with Entropy Weights

Hao Chen
Wuhan University of Technology
Chihua Lu
Wuhan University of Technology
Zhien Liu (lzen@whut.edu.cn)
Wuhan University of Technology
Cunrui Shen
Wuhan University of Technology
Menglei Sun
Wuhan University of Technology

Research Article

Keywords: automotive door, lightweight, Taguchi, grey relational analysis, entropy method, multi-objective optimisation

Posted Date: December 16th, 2021

DOI: https://doi.org/10.21203/rs.3.rs-1150153/v1

Multi-response Optimisation of Automotive Door using Grey Relational Analysis with Entropy Weights

Hao Chen[1,2], Chihua Lu[1,2], Zhien Liu[1,2,*], Cunrui Shen[1,2], Menglei Sun[1,2]

[1]*Foshan Xianhu Laboratory of the Advanced Energy Science and Technology Guangdong Laboratory, Foshan 528200, China*

[2]*Hubei Key Laboratory of Advanced Technology for Automotive Components, Wuhan University of Technology, Wuhan 430070, China*

Abstract: Tail-welded blanks (TWBs) are widely used in automotive bodies to improve structural performance and reduce weight. The stiffness and modal lightweight design optimisation of TWBs for automotive doors was performed in this study. The finite element model was validated through physical experiments. An L27 (3^{12}) Taguchi orthogonal array was used to collect the sample points. The multi-objective optimisation problem was transformed into a single-objective optimisation problem based on the grey relational degree. The optimal combination of structural design parameters was obtained for a tail-welded door using the proposed method; the weight of the door structure was reduced by 2.83 kg. The proposed optimisation method has fewer iterations and a lower computational cost, enabling the design of lightweight TWBs.

Keywords: automotive door; lightweight; Taguchi; grey relational analysis; entropy method; multi-objective optimisation

1. Introduction

Lightweight materials have become a popular research topic in the automotive industry in an effort to save energy and reduce exhaust emissions. There are two primary means of reducing automobile weight: lightweight materials [1-3] and lightweight structures [4-6]. Lightweight structures achieve weight reduction through the use of new structures. Lightweight materials include aluminium, magnesium alloy, and other materials with lower density, replacing traditional iron and steel materials in thin-walled panels to achieve weight reduction. Most thin-walled parts are stamped and welded from a single piece of material. The stamping die is large and the production cost is high. When the strength and stiffness requirements of the door are met, there are redundant materials, increasing the weight of the door, fuel consumption, and emissions.

TWB technology is widely used in the automobile industry; it can be used to compound parts, reduce the number of parts, and strengthen parts through the use of high-performance materials. Therefore, TWB technology integrates the advantages of traditional lightweight methods [7-9]. Chen et al. [10] employed parameter analysis and optimal design of thin-walled tube structures with TWB technology; the structural strength was improved, and the total weight was reduced by 10%.

The door assembly is an important part of an automobile; producing a lighter door structure that meets stiffness and noise, vibration and harshness (NVH) performance requirements is a key requirement. To reduce the weight of automotive doors, TWBs have become popular in automotive engineering [11-14]. Li et al. [15] proposed a lightweight automotive door design with a TWB structure in several load cases. Previous door optimisation designs only considered a single material, making it difficult to meet stiffness and dynamic requirements; the utilisation efficiency of the door material was not maximized.

Traditional discrete variable design optimisation methods such as the genetic algorithm and the particle swarm optimisation algorithm are expensive in terms of calculation cost for the automotive body system. The Taguchi method is an efficient and economical optimisation method that can greatly reduce the number of experimental tests and save time [16-18]. Liu et al. [19] established a multi-body dynamic model of a suspended monorail vehicle. The Taguchi method was used to determine the optimal combination of suspension parameters, which improved the lateral and vertical running stability of the vehicle. Shrestha et al. [20] studied the relationship between the print parameters and transverse rupture strength of sintered 316L stainless steel using the Taguchi method and determined the best additive manufacturing parameters to improve the transverse rupture strength. However, the structural optimisation of a door design must consider the stiffness, NVH, and weight of the door, indicating a multi-objective optimisation problem. A single Taguchi analysis is only applicable to single-objective optimisation, greatly limiting its application. Grey relational analysis with entropy weights can solve multi-objective optimisation problems with multiple criteria; its application in multi-objective problems has gained popularity [21-23]. She et al. [24] optimised the bending performance of optical fibres using grey relational analysis and found that the bending loss was reduced by an order of magnitude. Dabwan et al. [25] conducted experimental research on incremental sheet forming, using the grey relational method with entropy weights to determine the optimum process variables for single-point incremental forming. Most researchers use grey analysis for multi-objective optimisation without considering the robustness of the system, and combine it with Taguchi analysis.

In terms of door design variables, the discreteness of panel material types and the panel thicknesses are the most important features. However, few studies have focused on the structural stiffness of doors and NVH optimisation design considering discrete variables, and fewer studies have adopted grey relational analysis with entropy weights.

In this study, a finite element model of an automotive door was established. Orthogonal experiments were conducted using the Taguchi method by changing the panel thickness and panel material design variable combinations. Grey relational analysis and entropy weight were used to optimise the automotive door panel design, and the multi-objective optimisation problem was transformed into a single-objective optimisation problem. The optimised results, the significant influencing factors, and the optimal level combination were determined. The results show that the optimised structure reduces the weight to some extent, and the door performance meets baseline requirements; these findings provide guidance for the design of similar structures. Fig. 1 shows a flowchart of the proposed lightweight optimisation method.

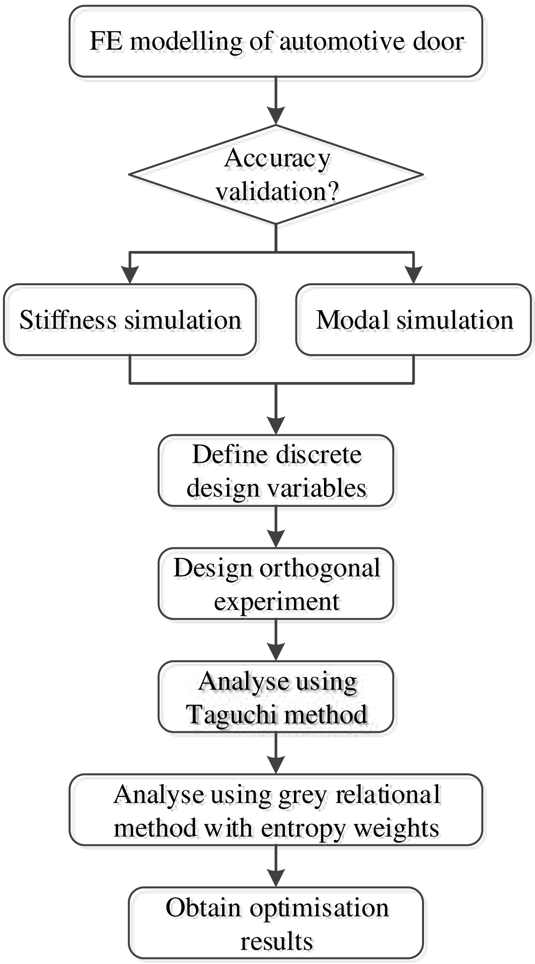

Fig. 1. Flowchart of lightweight optimisation method

2. Methodology

2.1 Taguchi method

The Taguchi method is an optimisation design method based on experimental design; the optimisation process is performed in accordance with experimental results. Selection of experimental parameters is the top priority in all optimisation studies [26]. Eq. (1) is often used to obtain the signal-to-noise ratio (S/N ratio) of 'the larger the better' response; Eq. (2) is used to obtain the S/N ratio of 'the smaller the better' response.

$$\eta_{Larger} = -10\lg\left(\frac{1}{m}\sum_{i=1}^{m}\frac{1}{y_{ij}^2}\right) \tag{1}$$

$$\eta_{Smaller} = -10\lg\left(\frac{1}{m}\sum_{i=1}^{m}y_{ij}^2\right) \tag{2}$$

2.2 Grey relational analysis with entropy weights

To optimise the door structure, the influence of the variables on the results must be understood. Grey relational theory effectively measures the influence of different variables. With the experimental data, grey relational theory determines the variables with the greatest influence. In addition to considering the influence of each variable on the objective function separately, grey relational theory can also consider the mutual influence of multiple variables [27-28].

As the dimensions and orders of magnitude of each evaluation index are different, each parameter must be normalised to eliminate the impact of different dimensions on the results. The normalisation method is usually described as follows:

For the larger the better response:

$$x_{ij}^{*}=\frac{x_{ij}-\min x_{j}}{\max x_{j}-\min x_{j}} \quad i=1,2,\cdots,m \; j=1,2,\cdots,n \tag{3}$$

For the smaller the better response:

$$x_{ij}^{*}=\frac{\max x_{j}-x_{ij}}{\max x_{j}-\min x_{j}} \quad i=1,2,\cdots,m \; j=1,2,\cdots,n \tag{4}$$

where x_{ij} and x_{ij}^{*} are the simulation and normalised values for the j^{th} response in the i^{th} trial, respectively; $\max x_j$ is the maximum value for the j^{th} response in all trials; $\min x_j$ is the minimum value for the j^{th} response in all trials; m is the number of trials, and n is the number of response indicators.

The normalised S/N ratio reference sequences and comparison sequences are used to calculate the grey relational coefficient of the S/N ratio for each quality characteristic:

$$\xi_{ij}=\frac{\max_{i}\max_{j}\Delta_{ij}+\rho\min_{i}\min_{j}\Delta_{ij}}{\Delta_{ij}+\rho\min_{i}\min_{j}\Delta_{ij}} \tag{5}$$

where ξ_{ij} is the correlation coefficient of the one-to-one correspondence between the comparison sequence and the reference sequence for the new data of the j^{th} response in the i^{th} trial in the grey relational analysis of influencing factors; $x_{ij}^{'}$ is the comparison sequence; $\Delta_{ij}=|x_{ij}^{*}-x_{ij}^{'}|$ is the absolute difference of the j^{th} response in the i^{th} trial; ρ is the grey relational resolution coefficient, whose value reflects the correlation integrity of each factor influencing the target value; generally, $\rho=0.5$.

To improve the evaluation accuracy of the grey relational analysis of factors influencing the target response value, the average correlation coefficient between each indicator factor in the new comparison sequence and the reference sequence is calculated as the grey relational degree.

$$\gamma_{ij}=\frac{1}{n}\sum_{j=1}^{n}\xi_{ij} \tag{6}$$

The weighted sum of the grey relational coefficients is the grey relational degree, calculated as

$$\gamma_{ij}=\sum_{j=1}^{n}\beta_{j}\xi_{ij}; \quad \sum_{j=1}^{n}\beta_{j}=1 \tag{7}$$

where β_j is the weight value of the j^{th} response variable.

With the different roles and influences of each response indicator, different weights must be assigned according to the importance of each indicator. The entropy weight method was used to assign weights to the target values.

The entropy weight method determines an objective weight according to the change in the response.

With a greater difference in response values, more information is provided, and a greater weight is assigned [29-30]. The weight calculation method based on the entropy value is as follows:

(1) Determine the geometric projection P_{ij} of each response:

$$P_{ij} = \frac{1 + x_{ij}^*}{\sum_{i=1}^{m}(1 + x_{ij}^*)} \tag{8}$$

(2) Calculate the entropy E_{ij}:

$$E_j = -\frac{1}{\text{In}m}\sum_{i=1}^{m} P_{ij}\text{In}P_{ij} \tag{9}$$

(3) Calculate the weight coefficient ω_j:

$$\omega_j = \frac{1 - E_j}{n - \sum_{j=1}^{n} E_j} \tag{10}$$

The weight coefficient reflects the amount of information in the index. An evaluation index may have different objective weights for different objects.

3. Finite element modelling and experiment validation for automotive door

3.1 Finite element modelling

The finite element model was pre-processed using HYPERWORKS; the model was computed using MSC.NASTRAN. The automotive door comprises thin-walled parts (including inner and outer panels, support panels, interior panels, and glass), meshed using shell elements with three or four nodes. To prevent the model stiffness from becoming inaccurately large, the number of three-node shell elements is restricted to not more than 3% of the elements in the finite element model. The automotive door structure is high-strength steel (Young's modulus $E = 2.1 \times 10^5$ MPa, mass density $\rho = 7.85 \times 10^3$ kg/m^3, Poisson's ratio $\mu = 0.3$, and no damping) and glass (Young's modulus $E = 6.9 \times 10^4$ MPa, mass density $\rho = 2.5 \times 10^3$ kg/m^3, Poisson's ratio $\mu = 0.3$, and no damping). Spot welding is used to connect the door parts, simulated with the element ACM2 (six-sided solid element and interpolation constraint element). The bonding material is adhesive (Young's modulus $E = 50$ MPa, mass density $\rho = 1.2 \times 10^3$ kg/m^3, Poisson's ratio $\mu = 0.49$, and damping coefficient $\zeta = 0.1$). There are 34186 elements and 981 three-node shell elements (2.87%) in the automotive door.

3.2 Experiment validation

There are differences between the finite element model of the door and the actual door; before structural optimisation of the door, the finite element model of the door must be verified. The correctness of the finite element model of the door is verified through a modal test and a stiffness test.

The automotive door must have sufficient stiffness and vibration resistance to ensure safety and comfort. To meet the energy savings and emission reduction requirements, the door must be lightweight.

Several indicators can be used to measure the stiffness of the door; the vertical sag stiffness, upper lateral stiffness, and lower lateral stiffness are important [31]. Three load cases are presented in Fig. 2. The vertical sag case is shown in Fig. 2. There are six degrees of freedom at the connection point between the hinge and the body (points P1 and P2), and two degrees of freedom in the translational direction of the door latch (point P3) along the y-direction (transverse direction of body). A force of 900 N in the direction of gravity was applied at point P3. The upper lateral case is shown in Fig. 2. There are six directional degrees of freedom, including 123456 degrees of freedom at the connection point between points P1 and P2, and three translational degrees (123 degrees of freedom) at point P3. A 900 N node force with two degrees-of-freedom was applied 5 mm below the edge line of the window frame in the upper left corner of the door inner panel. The lateral stiffness constraint conditions under the door are the same as those for upper lateral stiffness, but the applied load is different. The lower lateral case is shown in Fig. 2. A 900 N directional nodal force with two degrees-of-freedom was applied at the centre of the lower left corner of the inner panel of the door. The modal analysis of an automotive door considers its free mode. The first-order free mode of the door must meet certain requirements to prevent coupling resonance with the lower-order mode of the automotive body.

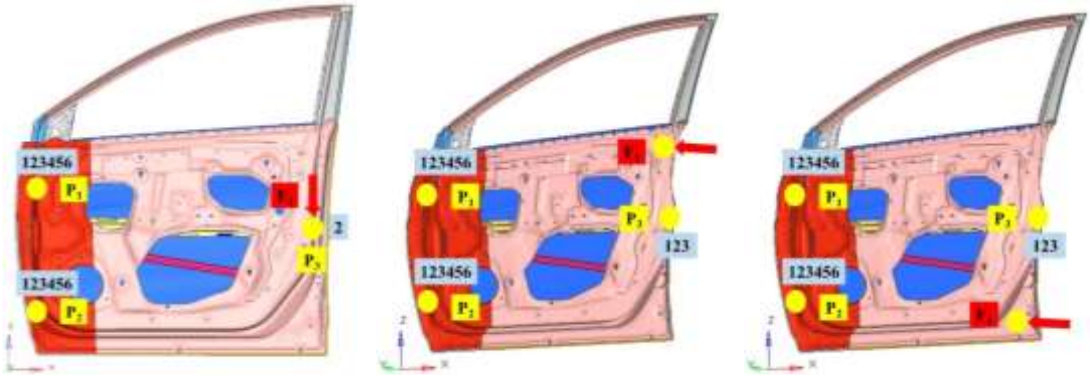

(a) Vertical sag (b) Upper lateral (c) Lower lateral

Fig. 2. Loading and boundary conditions for stiffness analysis of automotive door structure

Table 1. Comparison of FE simulations and experimental test

Parameter	Simulation	Experiment	Error (%)
Mass M (kg)	27.71	28.03	-1.14
Natural frequency f (Hz)	42.68	40.92	4.30
Vertical sag d_{sag} (mm)	1.64	1.67	-1.80
Upper lateral d_{upper} (mm)	1.03	1.06	-2.83
Lower lateral d_{lower} (mm)	13.28	13.36	-0.60

It is observed in Table 1 that the established finite element model can successfully predict the static and dynamic performance of the door structure with high precision, and can be used for subsequent parameter analysis.

4. Results and discussion

4.1 Design variables

The optimisation object is composed of six parts with different thicknesses and three parts with different material properties. The material types and thicknesses of each component were considered as independent discrete variables and divided into three levels for selection. The right inner panel, left inner panel, middle reinforcement of the inner panel, vertical belt reinforcement, outer panel, and transverse belt reinforcement have significant influences on the dynamic performance of the door, and are regarded as the optimisation object, as shown in Fig. 3. Three isotropic homogeneous materials were considered in this study: high-strength steel M1 (DP500), aluminium alloy M2 (ADC12), and magnesium alloy M3 (AM60). Their material properties are presented in Table 2. The range of each design variable is presented in Table 3.

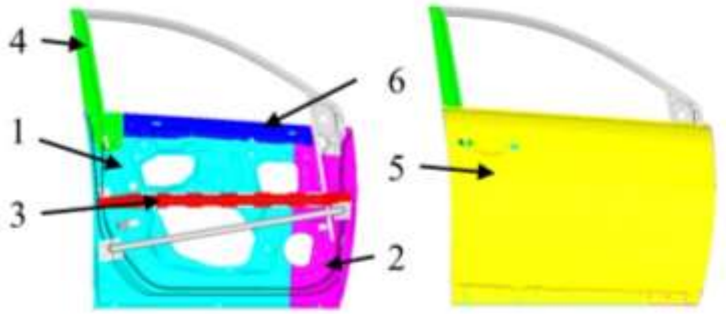

Fig. 3. Schematic of door parts: 1: right inner panel, 2: left inner panel, 3: middle reinforcement of inner panel, 4: vertical belt reinforcement, 5: outer panel, 6: transverse belt reinforcement

Table 2. Material properties of door structure

ID	Material	Elastic modulus (GPa)	Poisson's ratio	Density (kg/m^3)
1	Steel	210	0.30	7850
2	Aluminium	72	0.30	2770
3	Magnesium	45	0.33	1740

Table 3. Discrete design variables and corresponding values

Design variable	Value range
A (mm)	0.5, 0.7, 0.9
B (mm)	1.2, 1.4, 1.6
C (mm)	0.5, 0.6, 0.8
D (mm)	0.6, 0.8, 1.0
E (mm)	0.5, 0.7, 0.9
F (mm)	0.6, 0.8, 1.0
G	DP500, ADC12, AM60
H	DP500, ADC12, AM60
I	DP500, ADC12, AM60
J	DP500, ADC12, AM60
K	DP500, ADC12, AM60
L	DP500, ADC12, AM60

After determining the design variables, an orthogonal experiment with 12 factors and three levels was designed; an L27 (3^{12}) orthogonal array was selected, and values were assigned to the 12 design variables.

4.2 Analysis of S/N ratios

According to the quality characteristics, the results for multiple responses and the corresponding S/N ratios were calculated for the first-order natural frequency, the upper lateral stiffness displacement, the lower lateral stiffness displacement, and the mass, using Eqs. (1) and (2); the results are shown in Table 4.

Table 4. Simulation results and corresponding S/N ratios

NO.	d_{sag} (mm)	S/N	d_{upper} (mm)	S/N	d_{lower} (mm)	S/N	f (Hz)	S/N	M (kg)	S/N
1	2.411	-7.667	1.720	-4.858	1.06	-16.106	37.74	31.598	24.49	-27.833
2	6.571	-16.393	4.006	-12.213	2.33	-22.941	29.83	29.434	19.08	-25.647
3	10.070	-20.106	5.786	-15.409	3.22	-25.744	26.65	28.461	18.01	-25.142
4	4.786	-13.594	2.119	-6.628	1.49	-18.991	37.44	31.462	19.98	-26.032
5	6.771	-16.661	3.859	-11.890	2.11	-22.090	29.61	29.365	22.05	-26.966
6	2.303	-7.267	4.316	-12.884	2.44	-23.357	27.15	28.611	21.70	-26.770
7	5.115	-14.196	2.080	-6.484	1.39	-18.421	37.21	31.405	20.13	-26.092
8	1.922	-5.636	3.075	-9.930	2.51	-23.627	30.49	29.623	21.50	-26.661
9	3.637	-11.256	4.576	-13.388	2.41	-23.262	26.53	28.369	23.80	-27.649
10	2.672	-8.568	3.079	-9.939	1.86	-20.958	32.44	30.156	22.16	-26.976
11	6.107	-15.753	1.127	-1.154	0.92	-14.776	39.55	31.946	22.20	-26.943
12	9.520	-19.616	2.362	-7.615	1.70	-20.178	37.19	31.335	19.30	-25.739
13	5.049	-14.064	3.088	-9.940	2.30	-22.770	32.89	30.278	18.70	-25.456
14	6.331	-16.075	1.318	-2.510	0.82	-13.844	37.02	31.360	24.92	-28.003
15	1.957	-5.840	2.514	-8.152	1.41	-18.540	36.24	31.111	21.73	-26.782
16	5.394	-14.661	3.277	-10.464	2.28	-22.725	32.65	30.214	18.53	-25.383
17	1.554	-3.768	1.335	-2.399	0.89	-14.446	41.41	32.304	23.81	-27.551
18	3.264	-10.315	1.959	-6.009	1.31	-17.953	37.54	31.417	24.28	-27.807
19	2.427	-7.725	1.628	-4.373	1.10	-16.428	37.62	31.601	22.99	-27.289
20	6.329	-16.065	2.398	-7.737	1.65	-19.940	37.62	31.427	19.67	-25.915
21	9.229	-19.345	1.121	-0.966	0.80	-13.580	38.94	31.810	22.62	-27.095
22	4.780	-13.585	1.903	-5.693	1.49	-18.813	41.73	32.424	19.27	-25.709
23	6.554	-16.377	1.844	-5.485	1.49	-19.150	38.99	31.742	22.34	-27.065
24	1.702	-4.618	0.906	0.841	0.60	-11.138	43.36	32.725	25.50	-28.156
25	5.106	-14.180	1.687	-4.657	1.35	-18.158	40.96	32.332	19.82	-25.970
26	1.771	-4.913	2.337	-7.510	1.56	-19.372	38.06	31.536	20.82	-26.386
27	3.022	-9.641	0.986	0.087	0.57	-10.601	38.03	31.595	27.52	-28.876

A level with a large S/N ratio is the optimal parameter level. Fig. 4 shows the optimal horizontal combination of parameters in a single response. The best combination for d_{sag} is $A_3B_3C_1D_1E_3F_1G_1H_1I_3J_3K_1L_1$. The best combination for d_{upper} is $A_3B_3C_1D_3E_2F_3G_1H_1I_3J_1K_1L_3$. The best combination for d_{lower} is $A_3B_3C_1D_1E_3F_3G_1H_1I_3J_2K_1L_1$. The best combination for the first-order natural frequency f is $A_3B_2C_1D_3E_1F_1G_1H_1I_3J_1K_2L_1$. The best combination for the mass is

$A_1B_1C_1D_1E_1F_1G_3H_3I_3J_3K_3L_3$. The best combination for the mass is the material grade with the minimum thickness and density, which is consistent with actual conditions. According to the analysis, the optimal parameter combinations are different for different responses. Multi-objective optimisation is required to meet the objectives of minimum mass, maximum stiffness, and maximum modal frequency.

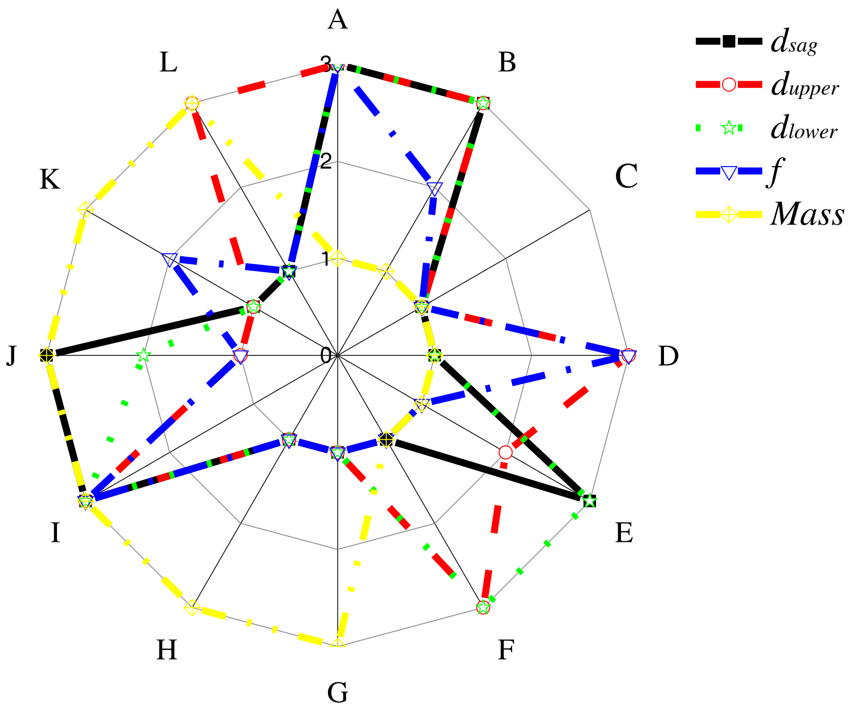

Fig. 4. Single-objective optimisation for each response

4.3 Analysis of grey relational

Using grey relational analysis, performance indicators of an automotive door can be transformed into a grey relational degree for comparative analysis to determine the optimal scheme.

Before grey relational analysis, the calculated S/N ratios for each response value were normalised to eliminate the influence of the dimension on the analysis. The experimental results were normalised and scaled to [0, 1]; the normalised results for each response value were calculated according to Eqs. (3) and (4) and are shown in Table 5. A larger normalised value indicates better performance; a normalised value of 1 indicates the best performance.

Table 5. Normalization of S/N ratios (NOR) and grey relational coefficient (GRC) for each performance characteristic

NO.	d_{sag}		d_{upper}		d_{lower}		f		$Mass$	
	NOR	GRC	NOR	GRC	NOR	GRC	NOR	GRC	NOR	GRC
1	0.239	0.396	0.351	0.435	0.364	0.440	0.741	0.659	0.721	0.641
2	0.773	0.687	0.803	0.718	0.815	0.730	0.245	0.398	0.135	0.366
3	1.000	1.000	1.000	1.000	1.000	1.000	0.021	0.338	0.000	0.333
4	0.601	0.556	0.460	0.481	0.554	0.529	0.710	0.633	0.238	0.396
5	0.789	0.703	0.783	0.698	0.759	0.674	0.229	0.393	0.489	0.494
6	0.214	0.389	0.845	0.763	0.842	0.760	0.056	0.346	0.436	0.470

7	0.638	0.580	0.451	0.477	0.516	0.508	0.697	0.623	0.254	0.401
8	0.114	0.361	0.663	0.597	0.860	0.781	0.288	0.412	0.407	0.457
9	0.458	0.480	0.876	0.801	0.836	0.753	0.000	0.333	0.671	0.603
10	0.294	0.415	0.663	0.598	0.684	0.613	0.410	0.459	0.491	0.496
11	0.734	0.652	0.123	0.363	0.276	0.408	0.821	0.737	0.482	0.491
12	0.970	0.943	0.520	0.510	0.632	0.576	0.681	0.611	0.160	0.373
13	0.630	0.575	0.663	0.598	0.804	0.718	0.438	0.471	0.084	0.353
14	0.753	0.670	0.206	0.386	0.214	0.389	0.687	0.615	0.766	0.681
15	0.127	0.364	0.553	0.528	0.524	0.512	0.629	0.574	0.439	0.471
16	0.667	0.600	0.696	0.622	0.801	0.715	0.424	0.464	0.065	0.348
17	0.000	0.333	0.199	0.384	0.254	0.401	0.903	0.838	0.645	0.585
18	0.401	0.455	0.422	0.464	0.485	0.493	0.700	0.625	0.714	0.636
19	0.242	0.398	0.321	0.424	0.385	0.448	0.742	0.660	0.575	0.540
20	0.753	0.669	0.528	0.514	0.617	0.566	0.702	0.627	0.207	0.387
21	0.953	0.915	0.111	0.360	0.197	0.384	0.790	0.704	0.523	0.512
22	0.601	0.556	0.402	0.455	0.542	0.522	0.931	0.879	0.152	0.371
23	0.772	0.687	0.389	0.450	0.565	0.534	0.774	0.689	0.515	0.508
24	0.052	0.345	0.000	0.333	0.035	0.341	1.000	1.000	0.807	0.722
25	0.637	0.580	0.338	0.430	0.499	0.500	0.910	0.847	0.222	0.391
26	0.070	0.350	0.514	0.507	0.579	0.543	0.727	0.647	0.333	0.429
27	0.359	0.438	0.046	0.344	0.000	0.333	0.741	0.659	1.000	1.000

The grey relational coefficient and the mean grey relational degree are calculated according to Eqs. (5), (6), and (7); the results are presented in Table 6. As the grey relational degree increases, the factors are closer to the optimal combination. The mean value of the grey relational degree also indicates the optimal parameter combination index. When the mean value of the grey relational degree corresponding to a factor level is the largest, its corresponding performance response is the best.

It is observed that H has the greatest influence on d_{sag} (Δ=0.4469), followed by B (Δ=0.1900), from the ranking of the mean grey relational degrees of different factor levels. Of the factors that affect d_{upper}, the effects of G and A are significant, with ranges of Δ=0.3240 and Δ=0.2705, respectively. Of the factors that affect d_{lower}, the effects of G and A are significant, with ranges of Δ=0.3262 and Δ=0.2298, respectively. A has the greatest influence on the first-order natural frequency f (Δ=0.2680), followed by G (Δ=0.1138). In terms of weight reduction, K has the greatest influence (Δ=0.2431), followed by G (Δ=0.1972), indicating that the material properties have a greater influence than the panel thickness.

Table 6. Mean grey relational degree at each level for each factor in automotive door TWB structure

Factor		A	B	C	D	E	F	G	H	I	J	K	L
d_{sag}	Level1	0.6255	0.5452	0.6510	0.6444	0.6396	0.6449	0.6630	0.8952	0.6370	0.6346	0.6626	0.6482
	Level2	0.6441	0.6442	0.6369	0.6406	0.6296	0.6403	0.6387	0.5810	0.6407	0.6436	0.6400	0.6342

	Level3	0.6549	0.7351	0.6365	0.6395	0.6553	0.6393	0.6228	0.4483	0.6468	0.6463	0.6219	0.6420
	Δ	0.0293	0.1900	0.0145	0.0049	0.0257	0.0055	0.0402	0.4469	0.0098	0.0117	0.0407	0.0140
	Rank	5	2	7	12	6	11	4	1	10	9	3	8
d_{upper}	Level1	0.5183	0.6563	0.6680	0.6518	0.6551	0.6660	0.8448	0.6756	0.6649	0.6932	0.6830	0.6649
	Level2	0.6794	0.6618	0.6629	0.6561	0.6687	0.6526	0.6210	0.6611	0.6543	0.6554	0.6597	0.6528
	Level3	0.7888	0.6685	0.6557	0.6787	0.6627	0.6680	0.5208	0.6499	0.6674	0.6380	0.6438	0.6689
	Δ	0.2705	0.0121	0.0123	0.0269	0.0136	0.0154	0.3240	0.0257	0.0131	0.0552	0.0391	0.0161
	Rank	2	12	11	5	9	8	1	6	10	3	4	7
d_{lower}	Level1	0.4881	0.6040	0.6134	0.6193	0.5819	0.6035	0.7987	0.6362	0.6111	0.6085	0.6545	0.6149
	Level2	0.6224	0.6109	0.6113	0.6062	0.6046	0.6105	0.5571	0.6044	0.6028	0.6118	0.6052	0.6062
	Level3	0.7179	0.6135	0.6038	0.6029	0.6419	0.6144	0.4726	0.5879	0.6146	0.6081	0.5687	0.6073
	Δ	0.2298	0.0095	0.0096	0.0164	0.0600	0.0110	0.3262	0.0484	0.0118	0.0037	0.0859	0.0087
	Rank	2	10	9	6	4	8	1	5	7	12	3	11
f	Level1	0.4370	0.5403	0.6285	0.5422	0.5884	0.5934	0.6781	0.5926	0.5520	0.5726	0.5305	0.6133
	Level2	0.5668	0.5958	0.5570	0.5551	0.5661	0.5275	0.5643	0.5637	0.5761	0.5666	0.5939	0.5563
	Level3	0.7049	0.5726	0.5232	0.6114	0.5542	0.5879	0.4663	0.5524	0.5806	0.5695	0.5843	0.5391
	Δ	0.2680	0.0554	0.0716	0.0693	0.0222	0.0659	0.1138	0.0289	0.0286	0.0061	0.0635	0.0570
	Rank	1	8	3	4	11	5	2	9	10	12	6	7
Mass	Level1	0.6411	0.6477	0.6361	0.6409	0.6815	0.6105	0.4934	0.5126	0.6137	0.5727	0.4592	0.5977
	Level2	0.6086	0.5950	0.5943	0.5924	0.5796	0.6080	0.6351	0.6306	0.5861	0.6195	0.6577	0.5967
	Level3	0.5695	0.5765	0.5887	0.5860	0.5580	0.6008	0.6906	0.6759	0.6193	0.6270	0.7023	0.6248
	Δ	0.0715	0.0712	0.0474	0.0549	0.1235	0.0097	0.1972	0.1633	0.0332	0.0543	0.2431	0.0280
	Rank	5	6	9	7	4	12	2	3	10	8	1	11

The entropy weight method is an objective method of value assignment that measures the relative importance of the indicators according to the uncertainty of each indicator. According to the grey relational coefficients in Eqs. (8), (9), (10), and Table 6, the weight values for d_{sag}, d_{upper}, d_{lower}, f, and *mass* are 0.1744, 0.1696, 0.2087, 0.2360, and 0.2113, respectively, representing their importance to the target value. The optimal solution is determined according to the grey relational degree.

The influence of the door design parameters is shown in Fig. 5. The maximum mean values of the grey relational degree for A, B, C, D, E, F, G, H, I, J, K, and L can be expressed as A_3, B_3, C_1, D_3, E_1, F_1, G_1, H_1, I_3, J_2, K_2, and L_1, respectively. Thus, the best combination of door structural design parameters is $A_3B_3C_1D_3E_1F_1G_1H_1I_3J_2K_2L_1$. The thicknesses of the right inner panel, left inner panel, middle reinforcement panel of the inner panel, window frame vertical reinforcement panel, outer panel, and window frame horizontal reinforcement panel are 0.9 mm, 1.6 mm, 0.5 mm, 1.0 mm, 0.5 mm, and 0.6 mm, respectively. The right inner panel, left inner panel, and window frame horizontal reinforcement panel were high-strength steel; the window frame vertical reinforcement panel and the outer panel were aluminium alloy, and the middle reinforcement panel of the inner panel was magnesium alloy.

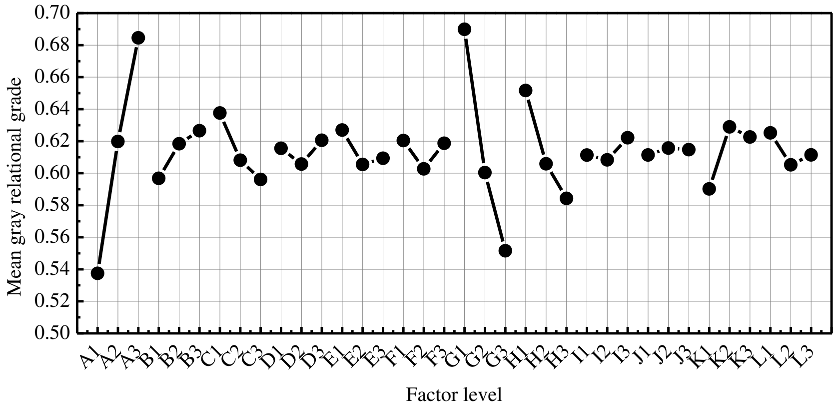

Fig. 5. Main effects of factor levels

The optimal combination of parameters was assigned to the finite element model for simulation analysis, and the final structural weight and dynamic performance parameters of the door were calculated, as shown in Table 7. With lightweight design, the weight of the door structure was reduced by 2.83 kg. The performance of the door increases and decreases, but meets all baseline design requirements.

Table 7. Comparison of door weight and dynamic performance before and after optimisation

Parameter	Initial design	Optimal design	Variation
Mass M (kg)	27.71	24.88	-10.21%
Natural frequency f (Hz)	42.68	42.30	-0.89%
Vertical sag d_{sag} (mm)	1.64	1.48	-9.76%
Upper lateral d_{upper} (mm)	1.03	1.04	0.97%
Lower lateral d_{lower} (mm)	2.21	2.39	8.14%

5. Conclusions

In this study, the lightweight TWB structure of an automotive door was considered as the research object. Through finite element analysis, the dynamic performance and lightweight indicators of the automotive door were obtained; the accuracy of the finite element model was verified through experiments. The main conclusions are presented as follows.

(1) A multi-objective discrete optimisation design was successfully developed through grey relational analysis of the S/N ratio. With only 27 iterations, this method is a discrete optimisation design with low computational cost and cost-effectiveness. Thus, it is more suitable than conventional methods for complex optimisation problems.

(2) The grey relational method is feasible for optimisation. The Taguchi method and grey relational method were used to analyse the results. The number of experiments was reduced, and the influence of each parameter on the results was measured. The entropy weight method was used to obtain the weight value of each target response and determine the optimal combination of structural parameters. Grey relational analysis with entropy weights can significantly improve the comprehensive structure performance.

(3) The optimisation results indicate that the weight of the door structure was reduced by 2.83 kg. The performance of the door increased and decreased, but met all baseline design requirements.

This method can effectively realise lightweight door design, and has a high value in engineering application.

Acknowledgements

This research work was supported by the National Natural Science Foundation of China (Grant No.52175111) and Foshan Xianhu Laboratory of the Advanced Energy Science and Technology Guangdong Laboratory (Grant No. XHD2020-003). The authors would like to express their appreciations for the above fund supports.

References:

[1] V. Volpe, S. Lanzillo, G. Affinita, B. Villacci, I. Macchiarolo, R. Pantani, Lightweight High-Performance Polymer Composite for Automotive Applications, POLYMERS-BASEL, 11 (2019).

[2] J. Lee, B. Min, J. Park, D. Kim, B. Kim, D. Ko, Design of Lightweight CFRP Automotive Part as an Alternative for Steel Part by Thickness and Lay-Up Optimization, MATERIALS, 12 (2019).

[3] Y. Jung, S. Lim, J. Kim, S. Min, Lightweight design of electric bus roof structure using multi-material topology optimisation, STRUCT MULTIDISCIP O, 61 (2020) 1273-1285.

[4] C. Wang, D. Wang, S. Zhang, Design and application of lightweight multi-objective collaborative optimization for a parametric body-in-white structure, P I MECH ENG D-J AUT, 230 (2016) 273-288.

[5] F. Xu, X. Wan, Y. Chen, Design optimization of thin-walled circular tubular structures with graded thickness under later impact loading, INT J AUTO TECH-KOR, 18 (2017) 439-449.

[6] J. Wang, Y. Zhang, N. He, C. Wang, Crashworthiness behavior of Koch fractal structures, MATER DESIGN, 144 (2018) 229-244.

[7] F. Pan, P. Zhu, Y. Zhang, Metamodel-based lightweight design of B-pillar with TWB structure via support vector regression, COMPUT STRUCT, 88 (2010) 36-44.

[8] G.Y. Sun, F.X. Xu, G.Y. Li, Q. Li, Crashing analysis and multiobjective optimization for thin-walled structures with functionally graded thickness, INT J IMPACT ENG, 64 (2014) 62-74.

[9] F. Panzer, M. Schneider, M. Werz, S. Weihe, Friction stir welded and deep drawn multi-material tailor welded blanks, MATER TEST, 61 (2019) 643-651.

[10] Y. Chen, F. Xu, S. Zhang, K. Wu, Z. Dong, Discrete Optimization Design of Tailor-Welded Blanks (TWBs) Thin-Walled Structures Under Dynamic Crashing, INT J AUTO TECH-KOR, 20 (2019) 265-275.

[11] K. Lee, D. Kang, Structural optimization of an automotive door using the kriging interpolation method, P I MECH ENG D-J AUT, 221 (2007) 1525-1534.

[12] J. Fang, Y. Gao, G. Sun, C. Xu, Q. Li, Multiobjective sequential optimization for a vehicle door using hybrid materials tailor-welded structure, P I MECH ENG C-J MEC, 230 (2016) 3092-3100.

[13] P. Zhu, Y. Shi, K. Zhang, Z. Lin, Optimum design of an automotive inner door panel with a tailor-welded blank structure, P I MECH ENG D-J AUT, 222 (2008) 1337-1348.

[14] F. Xu, S. Zhang, K. Wu, Z. Dong, Multi-response optimization design of tailor-welded blank (TWB) thin-walled structures using Taguchi-based gray relational analysis, THIN WALL STRUCT, 131 (2018) 286-296.

[15] G. Li, F. Xu, X. Huang, G. Sun, Topology Optimization of an Automotive Tailor-Welded Blank Door, J MECH DESIGN, 137 (2015).

[16] N. Mohamad, M. Wee, M. Mohamed, A. Hamzah, P. Menon, Multi-response optimization of chromium/gold-based nanofilm Kretschmann-based surface plasmon resonance glucose sensor using finite-difference time-domain and Taguchi method, NANOMATER NANOTECHNO, 10 (2020).
[17] L. Gao, A. Adesina, S. Das, Properties of eco-friendly basalt fibre reinforced concrete designed by Taguchi method, CONSTR BUILD MATER, 302 (2021).
[18] X. Sun, Z. Shi, J. Zhu, Multiobjective Design Optimization of an IPMSM for EVs Based on Fuzzy Method and Sequential Taguchi Method, IEEE T IND ELECTRON, 68 (2021) 10592-10600.
[19] W. Liu, Y. Yang, R. Zheng, P. Wang, Robust Optimization for Suspension Parameters of Suspended Monorail Vehicle Using Taguchi Method and Kriging Surrogate Model, J CHIN SOC MECH ENG, 40 (2019) 481-489.
[20] S. Shrestha, G. Manogharan, Optimization of Binder Jetting Using Taguchi Method, JOM-US, 69 (2017) 491-497.
[21] Q. Tran, V. Nguyen, S. Huang, Drilling Process on CFRP: Multi-Criteria Decision-Making with Entropy Weight Using Grey-TOPSIS Method, APPL SCI-BASEL, 10 (2020).
[22] D.F. Wang, S.H. Li, C. Xie, Crashworthiness optimisation and lightweight for front-end safety parts of automobile body using a hybrid optimisation method, INT J CRASHWORTHINES, (2021).
[23] Z.H. Wang, P.X. Yang, H. Peng, C. Li, C.N. Yue, W.J. Li, X.F. Jiang, Comprehensive evaluation of 47 tea [Camellia sinensis (L.) O. Kuntze] germplasm based on entropy weight method and grey relational degree, GENET RESOUR CROP EV, (2021).
[24] Y. She, W. Zhang, G. Liang, Y. Tang, S. Tu, Optimal design of large mode area all-solid-fiber using a gray relational optimization technique, OPTIK, 242 (2021).
[25] A. Dabwan, A.E. Ragab, M.A. Saleh, A.M. Ghaleb, M.Z. Ramadan, S.H. Mian, T.M. Khalaf, Multiobjective optimization of process variables in single-point incremental forming using grey relational analysis coupled with entropy weights, P I MECH ENG L-J MAT, (2021).
[26] T. Yuvaraj, P. Suresh, Analysis of EDM Process Parameters on Inconel 718 Using the Grey-Taguchi and Topsis Methods, STROJ VESTN-J MECH E, 65 (2019) 557-564.
[27] R. Rao, V. Yadava, Multi-objective optimization of Nd:YAG laser cutting of thin superalloy sheet using grey relational analysis with entropy measurement, OPT LASER TECHNOL, 41 (2009) 922-930.
[28] X. Zhang, F. Jin, P. Liu, A grey relational projection method for multi-attribute decision making based on intuitionistic trapezoidal fuzzy number, APPL MATH MODEL, 37 (2013) 3467-3477.
[29] F.H. Lotfi, R. Fallahnejad, Imprecise Shannon's Entropy and Multi Attribute Decision Making, ENTROPY-SWITZ, 12 (2010) 53-62.
[30] F. Xiong, D. Wang, Z. Ma, T. Lv, L. Ji, Lightweight optimization of the front end structure of an automobile body using entropy-based grey relational analysis, P I MECH ENG D-J AUT, 233 (2019) 917-934.
[31] X. Cui, S. Wang, S.J. Hu, A method for optimal design of automotive body assembly using multi-material construction, MATER DESIGN, 29 (2008) 381-387.